Journal of Human Evolution xxx (xxxx) xxx

Contents lists available at ScienceDirect

Journal of Human Evolution

journal homepage: www.elsevier.com/locate/jhevol

Early Upper Paleolithic human foot bones from Manot Cave, Israel

Sarah Borgel [a, b], Bruce Latimer [c, d], Yvonne McDermott [c, d], Rachel Sarig [b, e], Ariel Pokhojaev [a, b, e], Talia Abulafia [f], Mae Goder-Goldberger [f], Omry Barzilai [g], Hila May [a, b, *]

[a] Department of Anatomy and Anthropology, Sackler Faculty of Medicine, Tel Aviv University, PO Box 39040, Tel Aviv 6997801, Israel
[b] The Dan David Center for Human Evolution and Bio-history Research, The Shmunis Family Anthropology Institute, Sackler Faculty of Medicine, The Steinhardt Museum of Natural History; Tel Aviv University, PO Box 39040, Tel Aviv 6997801, Israel
[c] Department of Anatomy, Case Western Reserve University School of Medicine, Cleveland, OH 44106, USA
[d] Department of Orthodontics, Case Western Reserve University School of Dental Medicine, 10900 Euclid Avenue, Cleveland, OH 44106, USA
[e] Departments of Orthodontics and Oral Biology, The Maurice and Gabriela Goldschleger School of Dental Medicine, Sackler Faculty of Medicine, Tel Aviv University, Israel
[f] Department of Bible, Archaeology and Ancient Near East, Ben-Gurion University of the Negev, PO Box 653, Beer-Sheva 8410501, Israel
[g] Israel Antiquities Authority, PO Box 586, Jerusalem 91004, Israel

ARTICLE INFO

Article history:
Received 8 January 2019
Accepted 23 August 2019
Available online xxx

Keywords:
Pedal bones
Early Upper Paleolithic
Levant
Manot cave
Lisfranc's fracture

ABSTRACT

The transition from the Middle Paleolithic to the Upper Paleolithic in the Levant represents a major event in human prehistory with regards to the dispersal of modern human populations. Unfortunately, the scarcity of human remains from this period has hampered our ability to study the anatomy of Upper Paleolithic populations. This study describes and examines pedal bones recovered from the Early Upper Paleolithic period at Manot Cave, Israel, from 2014 to 2017. The Manot Cave foot bones include a partial, left foot skeleton comprising a talus, a calcaneus, a cuboid, a first metatarsal, a second metatarsal, a fifth metatarsal, and a hallucal sesamoid. All these remains were found in the same archaeological unit of the cave and belong to a young adult. Shape and size comparisons with Neanderthals, Anatomically Modern Human and modern human foot bones indicate a modern human morphology. In some characteristics, however, the Manot Cave foot bones display a Neanderthal-like pattern. Notably, the Manot Cave foot is remarkable in its overall gracility. A healed traumatic injury in the second metatarsal (Lisfranc's fracture) is most likely due to a remote impact to the dorsum of the foot. This injury, its subsequent debility, and the individual's apparent recovery suggest that the members of the Manot Cave community had a supportive environment, one with mutual responsibilities among the members.

1. Introduction

The Early Upper Paleolithic (EUP) (46-30 ka BP) in the Levant is a critical period of transition in human prehistory, since it is thought to reflect the interaction between modern human groups dispersing and the disappearance of Neanderthal populations in Eurasia (Bar-Yosef, 2002, 2007; Mellars, 2004, 2006; Hershkovitz et al., 2015; Hublin, 2015). However, despite the relatively abundant number of EUP sites in the Levant (e.g., Ksar Akil, Hayonim, Sefunim, Qafzeh, and Kebara), human remains are rare and, where they do exist, they are often fragmentary and without clear context (Bergman and Stringer, 1989; Gilead, 1991; Shea, 2007; Kuhn et al., 2009; Douka et al., 2013).

Manot Cave is a large active karstic cave (~1000 sq. meters) located in the western Galilee, Israel (Fig. 1A). Excavations at the site between 2010 and 2018 have yielded exceptionally well-preserved flint tools, human bones, faunal remains (primarily fallow deer and gazelle), as well as osseous industry and mollusks, indicating that the cave was inhabited from the late Middle Paleolithic (MP) to the EUP periods (Marder et al., 2013, 2018; Barzilai et al., 2016; Tejero et al., 2016; Alex et al., 2017). A partial modern human calvaria (MC-1), dated to ~55ka, indicates the simultaneous occupation of both modern humans and Neanderthals during the UP interface in the Levant (Hershkovitz et al., 2015). Among the human remains found at Manot Cave are several teeth (Sarig et al., 2019, in press) and several foot bones

* Corresponding author.
E-mail address: mayhila@tauex.tau.ac.il (H. May).

https://doi.org/10.1016/j.jhevol.2019.102668
0047-2484/

recovered from Area C (Fig. 1B, C). These units contain EUP assemblages with the Levantine Aurignacian and Early Ahmarian cultures (Marder et al., 2013; Barzilai et al., 2016; Tejero et al., 2016; Abulafia et al., submitted).

Owing to their natural fragility, human pedal remains are infrequently recovered from fossil assemblages. Therefore, the Manot Cave partial pedal skeleton adds novel information regarding early human physical activity levels and behavior. Additionally, the Manot Cave foot skeleton provides evidence regarding a remote pathological injury, which sheds light not only on the extent of physical activity the individual was involved in, but also implies the possible existence of social support systems and shared responsibilities among the Manot Cave inhabitants. Previous studies have examined early human foot bones in a functional context (DeSilva et al., 2019). These include observations relating to large muscular and ligamentous attachments and particularly the marked robusticity of the Neanderthal foot bones, all of which were presumed to reflect high levels of physical activity (Trinkaus, 1975; Trinkaus and Hilton, 1996; DeSilva et al., 2019). The active foraging lifestyle of Anatomically Modern Humans (AMH) was reflected in the relatively highly robust long bones of Ohalo II (Hershkovitz et al., 1995), yet they are more delicate than those of Neanderthals. The decrease in skeletal robusticity between Neanderthals and AMH has also been considered a climatic adaptation (Pearson, 2000). For example, both the abbreviated length and stoutness of the Neanderthal hallucal metatarsals (as compared to Late Pleistocene AMH) has been interpreted as an adaptation to cold environments (Betti et al., 2015). Since there are clear differences between the pedal anatomy of Neanderthals and AMH, an appreciation of morphological and metric variation of pedal remains can provide valuable taxonomic information (Trinkaus, 1975; Trinkaus and Hilton, 1996; Pablos et al., 2012, 2017).

Earlier studies have investigated various pathologies in fossil foot bones, providing insights into habitual stress levels and social interactions. AMH and Neanderthals were highly mobile populations and stresses imposed by long distance travels resulted in skeletal injuries, which temporarily impaired the mobility of the injured individual (Donahue and Sharkey, 1999; Donahue et al., 2000). Foot injuries and their subsequent debilities would probably have threatened the survival of, not only the affected

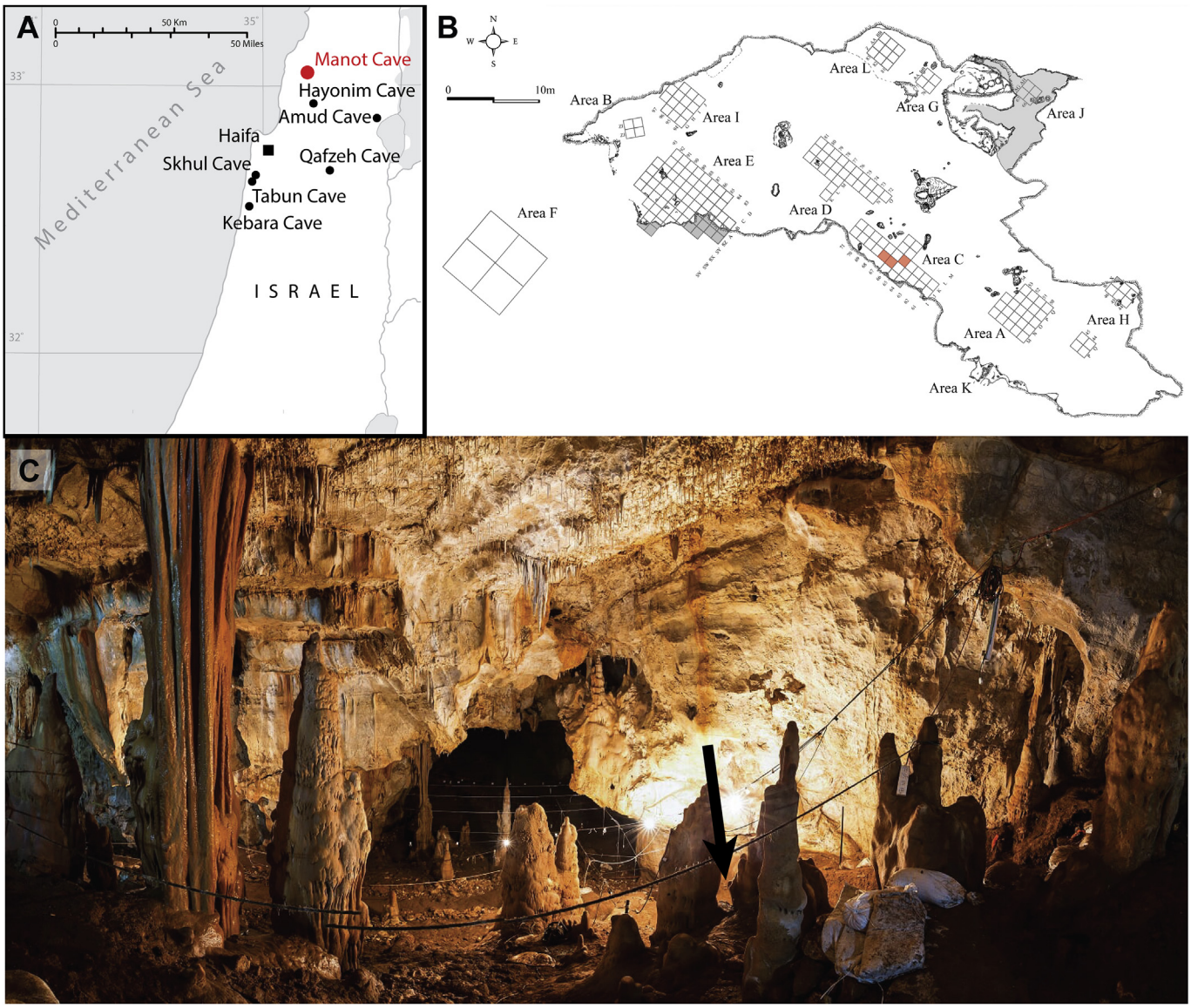

Figure 1. (A) Location of Manot Cave; (B) Map of the excavated areas in the cave, the orange squares in Area C indicating where the pedal remains were discovered and (C) Photograph of the entrance of the cave; Area C is situated at the bottom right side of the cave (black arrow).

Please cite this article as: Borgel, S et al., Early Upper Paleolithic human foot bones from Manot Cave, Israel, Journal of Human Evolution, https://doi.org/10.1016/j.jhevol.2019.102668

individual, but also the entire group. Evidence of healed foot injuries, such as a healed diaphyseal fracture on the fifth metatarsal of Shanidar 1 or the subtalar joint degeneration disease and arthritis of the Shanidar 3 ankle (Trinkaus and Zimmerman, 1982) were considered as evidence of altruistic support of the injured individual until their recovery. Other less serious conditions, such as a healed stress fracture of the fourth metatarsal of *Homo antecessor*, although not immediately life threatening, would nevertheless have hampered the affected individual's mobility (Martin-Francés et al., 2015).

The aims of the current study were to morphologically and metrically characterize the EUP foot bones found in Manot Cave, to investigate their population affiliations (Neanderthals vs. AMH and modern humans), and finally to examine the metatarsal injury and the potential insight it provides into the group's social structure and behavior.

2. Materials and methods

2.1. Materials

All pedal remains from Manot Cave belong to the left foot and include a talus (MC-14), a calcaneus (MC-2), a cuboid (MC-15), a first metatarsal (MC-18), a second metatarsal (MC-4), and a fifth metatarsal (MC-5), along with a single hallucal sesamoid bone (MC-11) (Fig. 2). All bones were revealed in Area C in close proximity to each other (Fig. 1, Supplementary Online Material [SOM], Table S1). Area C is situated at the base of the western talus of the cave, below Area E. The sediments of Area C consist of poorly sorted colluvium. The colluvium matrix is composed of terra rossa soil, angular rock fragments, and anthropogenic material (i.e., bone fragments, lithic artifacts marine mollusks, and charcoal particles). It is composed of eight stratigraphic Units that were described based on sedimentological criteria, and subsequently divided into two archaeological horizons that were defined based on the lithic assemblage techno-typological characteristics (Abulafia et al., submitted). Levantine Aurignacian was identified in Units 3, Unit 4 and upper Unit 5, and Ahmarian was identified in lower Unit 6 and Unit 7. The intermediate section, where the pedal bones were excavated, consists of lower Unit 5 and upper Unit 6 and contained a mixed archaeological assemblage of both Levantine Aurignacian and Ahmarian artifacts. This section also contained unique findings, including three marine mollusks; two Cowries shells (*Erosaria* sp. and *Zanaria pyrum*), a *Columbella rustica* shell, and four el-Wad points, two of which were made from non-local flint (Bar-Yosef Mayer, 2019; Abulafia et al., submitted).

Comparative material of pedal bones includes published data from various hominin groups, including Neanderthals, AMH, and modern humans (SOM Table S2).

2.2. Methods

The following descriptions of morphology and pathology were done using internationally accepted human anatomical terminology, with any deviation noted in the accompanying text. Although the Manot Cave human fossils are unusually well preserved, any post-mortem taphonomic damage is described in the SOM Table S3.

The determination that the elements derive from a single individual was based on the following criteria: the proximity of excavation localities, the size and side of the specimen, the correspondence of the matching articular surfaces, the adhering matrix and patina of the bones as well as the degree of bone mineralization. Age estimation was carried out based on comparisons with the state of the epiphyseal fusions in modern human pedal bones (Hoerr et al., 1962; Scheuer and Black, 2004; Cardoso and Severino, 2010). Stature was reconstructed using linear regression equations (sex unknown) using the talus, calcaneus (Holland, 1995), and the first and fifth metatarsals (Byers et al., 1989).

In addition, all the fossil pedal bones were CT scanned at Carmel Medical Center, Haifa, Israel (Philips iCT 256, Philips Medical Systems, Cleveland, Ohio: slice thickness 1 mm, voltage 80 kV, current 548 mA). The resulting scans were examined and analyzed using the "IntelliSpace Portal" (Radiology DICOM image processing applications software Version 8). To more accurately evaluate the pathology of the second metatarsal, this bone underwent additional X-ray and μCT scanning (Nikon XT H 225 ST: beam energy 80 kV, beam current 200uA, and power 16.0 W). CT and μCT images were processed using Amira 6.3 (Thermo Fischer Scientific, US).

All linear measurements were taken with digital calipers (Dijite, China, accuracy ±0.03 mm). Measurements of the foot bones followed those of Trinkaus (1975), Vandermeersch (1981), and Pablos et al. (2012, 2013, 2014 and 2017). These include 15 measurements and seven indices for the talus, eight measurements and five indices for the calcaneus, seven measurements and four indices for the cuboid, 10 measurements and five indices for the first metatarsal, and 10 measurements and four indices for the second and fifth metatarsals (SOM Table S4). In addition, four angles and three curvature radii were measured for the talus and two angles and two curvature radii measurements were collected for the calcaneus, following Barnett and Napier (1952), Day and Wood (1968), Latimer and Lovejoy (1989), DeSilva (2009), and Mahato and Murthy (2012) (SOM Fig. S1). The angular and curvature values were taken from photographs, using ImageJ 1.52a and SolidWorks (2016) software. All the photographs used in the metric analyses were carefully composed in an effort to minimize any angular distortion or parallax.

3. Morphological descriptions

3.1. MC-14 – left talus

In dorsal view (Fig. 2A), the lateral and medial margins of the trochlea converge slightly posteriorly to an acute angle of approximately 24° (SOM Fig. S1A). The medial and lateral trochlear walls are parallel and vertical. In medial view (Fig. 2A), the malleolar facet is typically comma-shaped and although the head of the comma extends onto the talar neck, it is only slightly cupped. The radius of curvature of the medial edge of the trochlea is ~13 mm (SOM Fig. S1B). However, this is only an estimate because of the erosional damage on the anteromedial edge of the trochlea. On the lateral side (Fig. 2A), the radius of curvature of the trochlea is approximately 15 mm (SOM Fig. S1C). This, combined with the previously mentioned medial curvature radius, demonstrates that the approximate central axis of the trochlear frustum ("the dorsiflexion axis") inclines relative to the trochlear surface at roughly 6° (SOM Fig. S1D). All these angular measurements fall within the range of modern humans (Day and Wood, 1968; Rhoads and Trinkaus, 1977; Latimer et al., 1987; DeSilva, 2009; Mahato and Murthy, 2012).

In posterior view, the sub-bursal groove for the tendon of flexor hallucis longus inclines downward in a plantarmedial direction. The medial and lateral walls of this groove are parallel and do not diverge superiorly. The lateral edge of this groove is notably sharp where it meets the posterior calcaneal articulation. In plantar view (Fig. 2A), the talar head presents a uniform curvature with a radius of approximately 15 mm (SOM Fig. S1E). The normally flattened area for the "spring ligament" is largely obliterated owing to postmortem erosional damage. The articular area for the medial calcaneal facet is separated from the posterior talar facet by the

Please cite this article as: Borgel, S et al., Early Upper Paleolithic human foot bones from Manot Cave, Israel, Journal of Human Evolution, https://doi.org/10.1016/j.jhevol.2019.102668

Figure 2. Early Upper Paleolithic foot remains from Manot Cave. (A) Left talus MC-14; (B) Left calcaneus MC-2; (C) Left first metatarsal MC-18; (D) Left second metatarsal MC-4; (E) Left fifth metatarsal MC-5; (F) Left cuboid MC-15, and (G) Hallucal sesamoid MC-1. The pedal bones are presented in four views: D - dorsal view; P - plantar view; L - Lateral view; and M– medial view.

sulcus tali with a breadth of 5 mm. The posterior calcaneal facet is ovoid in shape, with a sharp contour and the surface displays a slight sigmoidal twist along its long axis.

3.2. MC-2 – left calcaneus

In dorsal view (Fig. 2B), the long axis of the posterior talar facet is oriented obliquely to the bone's longest axial dimension with an angle of ~55° (SOM Fig. S1F). The radius of curvature of the posterior facet is ~30 mm (SOM Fig. S1H) and the number of subtended degrees is ~78° (SOM Fig. S1H). The anterior and middle talar facets are connected by a thin isthmus of subchondral bone, which gives the combined articular facet a tightly 'waisted' hourglass appearance. There is a slightly elevated crest on the anterolateral edge of the middle talar facet, but this does not divide the surface into two separate facets. The radius of curvature of the combined middle and anterior talar facets is ~36 mm (SOM Fig. S1G). The calcaneal tuber is stout with a thick, non-waisted body. In posterior view, the long axis of the main body of the tuber inclines such that its most dorsal margin is lateral to its most plantar segment. This axis through the tuber does not include the unusually large lateral plantar process. The insertion of the triceps surae tendon is horizontally oriented midway across the tuber. Although this well preserved bone is very similar to the typical “modern human” condition (DeSilva et al., 2019), one feature that does differ is the unusually large lateral plantar process (Fig. 3A). The lateral plantar process projects more towards the plantar surface than does the adjoining medial process. In plantar view, what is usually a cleft between the two processes, here is filled in with bone so that the most distal margin of the two processes is not bicornate (the usual condition in both modern humans and Neanderthals); however, it is a single elevated margin roughly perpendicular to the bone's proxodistal long axis (Fig. 3B).

In lateral view (Fig. 2B), the slightly elevated retrotrochlear eminence inclines anterosuperiorly from the large lateral plantar process to the moderately sized fibularis trochlea. There is a roughened area on the lateral side of the tuber for the attachment of the calcaneofibular ligament. The superomedial course of this ligament resulted in a polished, shallow concavity along the posterolateral margin of the posterior talar facet. Immediately anterior to this “cut-out” is a polished area of bone along the lateral margin of the posterior talar facet. This polish is attributed to the approximation of the combined tendons for the fibularis longus and brevis muscles. In medial view (Fig. 2B), the sustentaculum tali is robust and the sub-bursal groove for the flexor hallucis longus has a width of 16 mm. In anterior view, the facet for the cuboid is sigmoidally twisted with a “beak” that projects anteriorly on its superomedial margin. This beak-like extension is beneath the most distal margin of the anterior talar facet and the combined subchondral bone forms a sharp edge overhanging the cuboid articulation. This feature indicates an eccentrically placed axis of rotation, indicating the “locking” mechanism typically found in human calcaneocuboid articulations (DeSilva et al., 2019).

3.3. MC-15 – left cuboid

In dorsal view (Fig. 2C) this cuboid presents a typical trapezoidal profile, with its anterior and posterior edges converging laterally toward the groove for fibularis longus. The bone's proximal

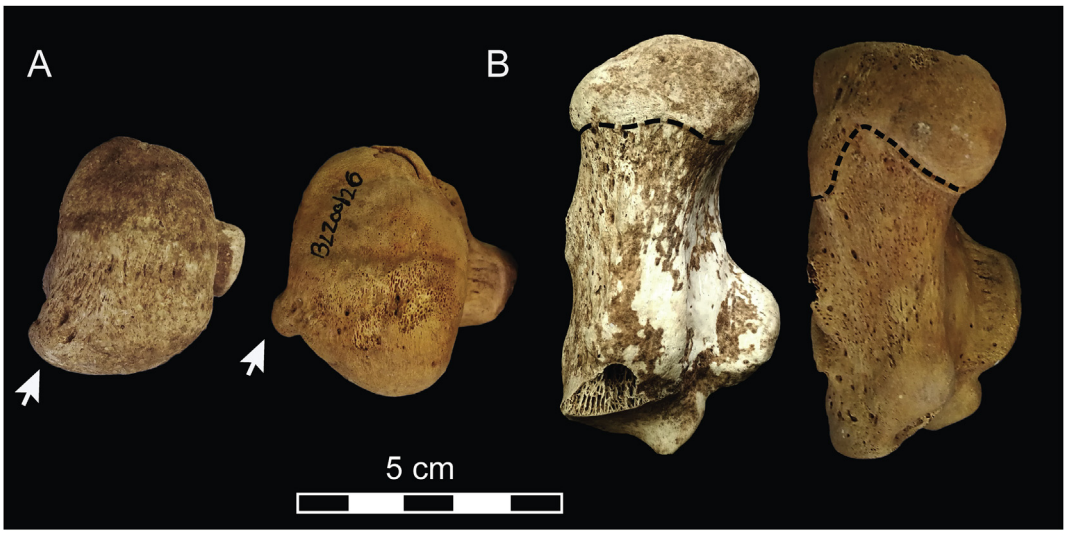

Figure 3. Comparison of the Manot Cave calcaneus (left) and a typical modern human (right). (A) Posterior view; the white arrow indicates the unusually large lateral tubercle in the Manot Cave specimen; (B) Plantar view, the black line between the lateral and medial tubercles shows the unusual non-bicornate shape in the Manot Cave calcaneus.

articular surface for the calcaneus is roughly triangular with a proximally projecting "beak" on its plantar angle. This projecting "beak" corresponds to a similar projection on the cuboid articular surface of the associated calcaneus (MC- 2). The fact that these projections are eccentric to the joint's center of rotation means that any significant rotational motion in the calcaneocuboid joint will "lock" as a stabilizing mechanism during the toe-off phase of human gait (Bojsen-Møller, 1979; Lovejoy et al., 2009; DeSilva et al., 2019). In medial view (Fig. 2C) there is a flattened articular surface for the lateral cuneiform. Meeting this joint is a small articular facet for the navicular. The navicular and cuneiform subchondral surfaces are continuous but are divided by a slightly raised, palpably rounded crest. The distal joint surface is roughly triangular and has a slightly raised elevation separating the facets for the fourth and fifth metatarsals. This articular topography matches that found in the fifth metatarsal (MC-5). As is usual in modern humans, the proximal shoulder of the groove for the fibularis tendon is more projecting than is the distal shoulder. In addition, the proximal shoulder is rubbed smooth by the fibularis longus tendon and its associated cartilaginous sesamoid.

3.4. MC-18 – left first metatarsal

The articular facet for the medial cuneiform is typically flat and reniform in outline, with a slight sigmoid twist along its dorsoplantar long axis (Figs. 2D, 4A). Immediately anterior to the hilus and in lateral view, there is a roughened, oval-shaped shallow depression marking the insertion of the fibularis longus tendon. Immediately dorsal to this muscle insertion is a shallow contact facet for the second metatarsal (MC-4). The shaft of the bone is triangular in cross-section and flares slightly at the metaphyseal junction with the head (Fig. 2D). The shaft is perforated in several areas by nutrient foramina. The articular surface of the head is typically "domed" (Fig. 2D), indicating the passive hyperextension of the metatarsophalangeal joint (Latimer and Lovejoy, 1990; DeSilva et al., 2019). The dorsal margin of the head is somewhat asymmetrical with the lateral edge progressing more proximally along the shaft (Figs. 2D, 4B). This latter observation is related to the rotation that occurs at this joint during toe-off. In distal perspective, the anterior "beak" of the articular head is confined on both sides by the two parallel sesamoidal grooves. The medial groove is slightly deeper than the lateral and the associated hallucal sesamoid (MC-11), which resided, in life, within the medial groove. On the dorsolateral and dorsomedial margins of the metatarsal head, there are rugose, rounded impressions that accommodate the collateral ligaments.

3.5. MC-4– left second metatarsal

The epiphyseal line between the metatarsal head and the diaphysis remains obvious and partially unfused. It is clearly apparent on the dorsum of the metatarsal head and on the lateral plantar cornu (Fig. 2E). Except for these marginal areas of non-fusion, the majority of the epiphysis is clearly synostosed to the diaphysis (Fig. 5). This metatarsal exhibits a minimal amount of torsion along its remarkably smooth diaphysis. The proximal articular surface is roughly triangular with a notch excavated immediately inferior to the facet for the adjacent third metatarsal. In life, this notch is occupied by an interosseous ligament; however, in this specimen it is distorted (see the Pathology section 4.5 below).

3.6. MC-5 – left fifth metatarsal

The epiphyseal line between the head and the shaft of this bone remains clearly evident (Fig. 2F). The plantar juncture was recently synostosted, whereas the epiphyseal line on the dorsum remains open and visible. In dorsal view, the shaft is bowed such that the outline of the shaft is concave laterally (Fig. 2F). There is no evidence for the attachment of the fibularis tertius muscle. The tuberosity and the proximal facets are unremarkable and are the same as the typical modern human condition. The articular surface for the cuboid exhibits a topography that conforms exactly to that of the associated cuboid (MC-15). The tuberosity and the groove for abductor digiti minimi are moderate in size. The metatarsal head is twisted relative to the base such that its long axis is oriented laterally (Fig. 2F).

3.7. MC-11 – hallucal sesamoid

This is a "typical" modern human hallucal sesamoid (Fig. 2G). It has a bifaceted articular surface and a roughened plantar surface. This sesamoid was articulated in life, with the first metatarsal MC-18.

Please cite this article as: Borgel, S et al., Early Upper Paleolithic human foot bones from Manot Cave, Israel, Journal of Human Evolution, https://doi.org/10.1016/j.jhevol.2019.102668

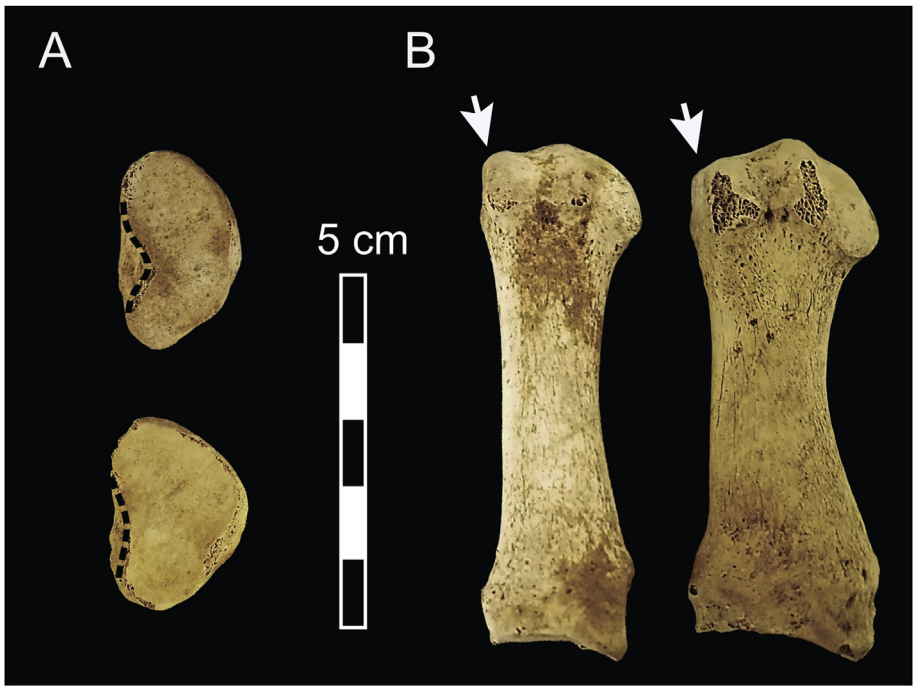

Figure 4. Comparison of the Manot Cave first metatarsal and a typical modern human. (A) Posterior view, the black line indicates the reniform shape of the proximal epiphysis, well defined in Manot Cave (upper specimen); (B) Plantar view, the white arrow indicates the dorsal margin of the head, asymmetrical in Manot Cave (left specimen).

4. Results

4.1. Minimum number of individuals

There are several lines of evidence to support the notion that all the pedal bones from Manot Cave belonged to the same individual: 1. They were found in the upper layers of Area C close to each other (Fig. 1B; SOM Table S1); 2. All bones are from the left foot; 3. All bones exhibit a similar color and taphonomic condition (Fig. 2); 4. The bone's corresponding articular surfaces match (Fig. 6); 5. All bones are of an equivalent developmental age; and 6. The unique finding next to the bones (marine shells and flint assemblage, see section 2.1 above) could possibly have originated from a single burial that partially slid down the talus (Abulafia et al., submitted).

4.2. Age estimation

The calcaneus and the first metatarsal are completely fused with no apparent epiphyseal line (Fig. 2B, D). The heads of the second and fifth metatarsals are nearly completely synostosed; however, margins of the epiphyseal lines remain apparent or partially unfused, most notably, on the dorsal and plantar sides (Fig. 2E, F). The complete fusion of the calcaneal apophysis and the first metatarsal epiphysis occurs at a minimum age of 15 years for both males and females. The nearly complete synostosis of the heads of the second and fifth metatarsals indicates an age between 13 and 17 years, depending on the sex of the individual (Hoerr et al., 1962; Scheuer and Black, 2004; Cardoso and Severino, 2010). The fact that the calcaneal apophysis and the hallucal metatarsal are fully synostosed, whereas the epiphyses of the two metatarsals are still partially unfused is not unusual (DeSilva et al., 2010) and may be considered as the normal condition in a significant portion of modern populations (Cardoso and Severino, 2010). Altogether, the incomplete synostoses of the heads of the second and fifth metatarsals and the complete fusion of the calcaneal apophysis and hallucal metatarsal suggest that this individual was between 15 and 17 years of age at the time of death.

4.3. Stature estimation

Based on the combined length of the talus and calcaneus (Holland, 1995), the height of the Manot Cave individual was 161.9 cm ± 5.02 cm. Based on the lengths of the first and fifth metatarsals (Byers et al., 1989), the height of the Manot Cave individual was 172.7 cm ± 6.50 cm (first metatarsal) and 169.9 cm ± 7.60 cm (fifth metatarsal).

4.4. Comparative analysis

All metric data for the pedal bones excavated at Manot Cave as well as the metric data for the comparative samples appear in SOM Tables S5–S10. All measurements are in mm unless otherwise specified.

Talus MC-14 The MC talus is shorter and narrower, compared with the other hominin groups (Fig. 7; SOM Table S5). Its height-to-length proportion falls within the AMH and modern human ranges of normal variation, whereas the height to breadth index (69.6) is within the Neanderthal range (68.8 ± 5.19, n = 12) and

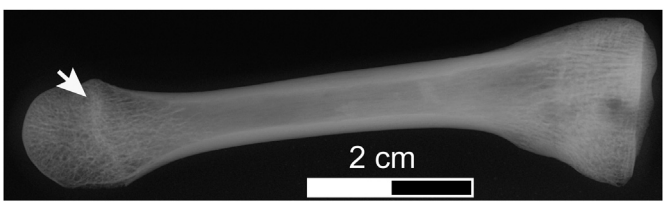

Figure 5. X-ray image of the Manot Cave left second metatarsal (MC-4); the white arrow points to the fusion line of the epiphysis.

Please cite this article as: Borgel, S et al., Early Upper Paleolithic human foot bones from Manot Cave, Israel, Journal of Human Evolution, https://doi.org/10.1016/j.jhevol.2019.102668

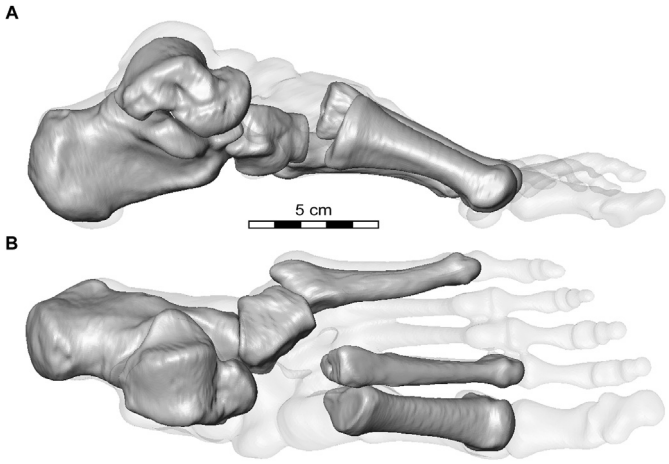

Figure 6. Three-dimensional reconstruction of the Early Upper Paleolithic Manot Cave foot in (A) medial view and (B) dorsal view. The Manot Cave pedal bones were placed based on a CT scan and a volume reconstruction of a modern human left foot.

outside the modern human range (56.9 ± 4.40, n = 40) (Fig. 7; SOM Table S5). The trochlea of MC-14 is relatively short but tall compared with Neanderthals, AMH, and modern humans (Fig. 7; SOM Table S5), whereas its breadth falls within the variation of the other hominin groups (SOM Table S5). The lateral malleolar facet height and breadth are within the range of the other hominin groups (SOM Table S5). The head (30.2 mm) is shorter than that of the Neanderthals (34.5 ± 3.21 mm, n = 13) and AMH (34.9 ± 3.13 mm, n = 7), but is similar to modern humans (32.5 ± 2.90 mm, n = 161), and its breadth is narrower, compared with all three groups (SOM Table S5). Nevertheless, the head breadth-to-length ratio is similar to that of both Neanderthals and AMH (SOM Table S5). The head-neck angle and head torsion angle fall within the range of all the hominin groups (SOM Table S5). The MC-14 posterior calcaneal articular facet length falls within the range of the other hominin groups, yet its breadth is smaller than the comparative samples, resulting in a smaller breadth-to-length ratio (63.6) than that of Neanderthals (71.8 ± 4.62, n = 13) and AMH (68.4 ± 3.93, n = 7) (SOM Table S5). Although in absolute values, the head neck length and the trochlear length are smaller than those of modern humans, relative to the total length of the talus, it is within their range.

Calcaneus MC-2 This bone's maximum length falls within the lower end of the ranges of variation of the other hominin groups (Fig. 7; SOM Table S6). It is, however, narrower (40 mm) compared with that of AMH (43.5 ± 2.16 mm), but it falls within the variation of Neanderthals (42.9 ± 4.25 mm, n = 10) and modern humans (40.0 ± 3.70 mm, n = 164). The width-to-length ratio (breadth index) falls within the range of other hominin groups (Fig. 7; SOM Table S6). MC-2 is taller (40.2 mm) than modern human calcanei (36.0 ± 3.50 mm, n = 164), but it falls within the ranges of variation of Neanderthals and AMH, as does its height-to-length proportion (SOM Table S6). The MC-2 body length (56.1 mm) is smaller than that of Neanderthals (61.8 ± 4.89 mm, n = 8) and is similar to AMH and modern humans. In addition, the MC-2 body length-to-total length (72.4) is similar to that of AMH (72.2 ± 2.15, n = 12) and modern humans (71.8 ± 2.90, n = 164), but smaller than the values obtained for the Neanderthals (75.7 ± 2.59, n = 7) (Fig. 7; SOM Table S6). The sustentacular breadth (16.9 mm) is larger than that of modern humans (14.2 ± 2.60 mm, n = 164) and falls within the range of Neanderthals (14.8 ± 3.31 mm, n = 9) and AMH (15.3 ± 2.83 mm, n = 8).

Cuboid MC-15 The medial and lateral lengths of this cuboid are similar to the AMH individual available for comparison (Skhul IV) and fall within the range of Neanderthals (Fig. 7; SOM Table S7). The MC-15 wedging index (51.8) falls within the higher limit of the Neanderthal's variation (46.0 ± 6.32, n = 6), yet it is smaller than the index in modern humans (62.1 ± 6.80, n = 40) (Fig. 7; SOM Table S7). The Manot Cave cuboid height (20.6 mm) is less than that of the Neanderthals (26.9 ± 2.95 mm, n = 6) and AMH (24.7 mm). The calcaneal articular height of MC-15 (19.5 mm) falls within the lower range of Neanderthals (21.6 ± 2.23 mm, n = 5), whereas the AMH specimen falls in the Neanderthal's upper range (23.0 mm). The calcaneal articular breadth is similar to that of the AMH specimen and falls within the ranges of both Neanderthals and modern humans (SOM Table S7). The calcaneal articular index of the Manot Cave cuboid (91.2) is within the range of Neanderthals (85.5 ± 18.80, n = 5) and modern humans (83.9 ± 9.60, n = 40) (Fig. 7, SOM Table S7), yet it is smaller than the AMH specimen (100). The metatarsal articular size of MC-15 as well as its index is smaller than those of all other hominin groups (SOM Table S7).

First metatarsal MC-18 This bone is longer (65.1 mm) than in the Neanderthals (55.9 ± 4.79 mm, n = 8) and AMH (60.7 ± 2.57 mm, n = 6), but it is within the modern human range (63.0 ± 4.50 mm, n = 40) (Fig. 8; SOM Table S8). Its midshaft dorsoplantar (DP) diameter (12.9 mm) is within the range of Neanderthals (12.3 ± 1.74 mm, n = 9) and modern humans (13.9 ± 1.50 mm, n = 47), yet its mediolateral (ML) diameter (12.4 mm) is smaller than in Neanderthals (14.6 ± 1.77 mm, n = 9) and AMH (14.9 ± 1.24 mm, n = 7), but within the range of modern humans (SOM Table S8). Its midshaft robusticity index (38.9) is smaller compared with the other hominin groups and has larger differences when compared with Neanderthals (48.5 ± 3.56, n = 8) and AMH (49.4 ± 2.44, n = 6) than with modern humans (42.2 ± 2.30, n = 40) (Fig. 8; SOM Table S8). The size of the proximal articular surface is relatively small, yet within the range of the other hominin groups. The proximal articular ratio falls within the range of the other groups (SOM Table S8). The distal end of the bone is small compared with other hominin groups, as is its distal articular ratio (Fig. 8; SOM Table S8).

Second metatarsal MC-4 The length of MC-4 (76.5 mm) is smaller than that of AMH (80.8 ± 1.77 mm, n = 2) and is in the range of Neanderthals and modern humans (Fig. 8; SOM Table S9). The DP (8.2 mm) and ML (6.9 mm) diameters are smaller than those of Neanderthals (DP = 9.5 ± 0.98 mm, n = 9 and ML = 8.0 ± 1.09 mm, n = 8) and AMH (DP = 11.6 ± 2.08 mm, n = 3 and ML = 8.7 ± 0.32 mm, n = 3), but fall within the range of modern humans (DP = 8.8 ± 1.00 mm, n = 153 and ML = 7.5 ± 1.00 mm, n = 153). The MC-4 metatarsal is more gracile compared with that of the other hominin groups (Fig. 8, SOM Table S9). The height of the proximal epiphysis and proximal articular surface of the Manot Cave second metatarsal falls within the ranges of the other hominin groups, but they are narrower (SOM Table S9). The proximal articular index of the Manot Cave second metatarsal (40.3) falls within the range of Neanderthals (43.3 ± 5.31, n = 3) and AMH (40.2), but is smaller than that of modern humans (46.1 ± 2.50, n = 40) (SOM Table S9). The height of MC-4 falls within the range of Neanderthals and modern humans yet is smaller than that of AMH (SOM Table S9). Breadth measurements of the distal epiphysis of MC-4 are smaller than the other hominin groups. The articular index, however, is smaller than that of Neanderthals and modern humans, yet it is within the range of AMH (Fig. 8; SOM Table S9).

Fifth metatarsal MC-5 This bone is longer (70.4 mm) than the modern human fifth metatarsal (63.4 ± 3.50 mm, n = 40), yet falls within the variation of the Neanderthals (68.2 ± 4.13 mm, n = 5)

Please cite this article as: Borgel, S et al., Early Upper Paleolithic human foot bones from Manot Cave, Israel, Journal of Human Evolution, https://doi.org/10.1016/j.jhevol.2019.102668

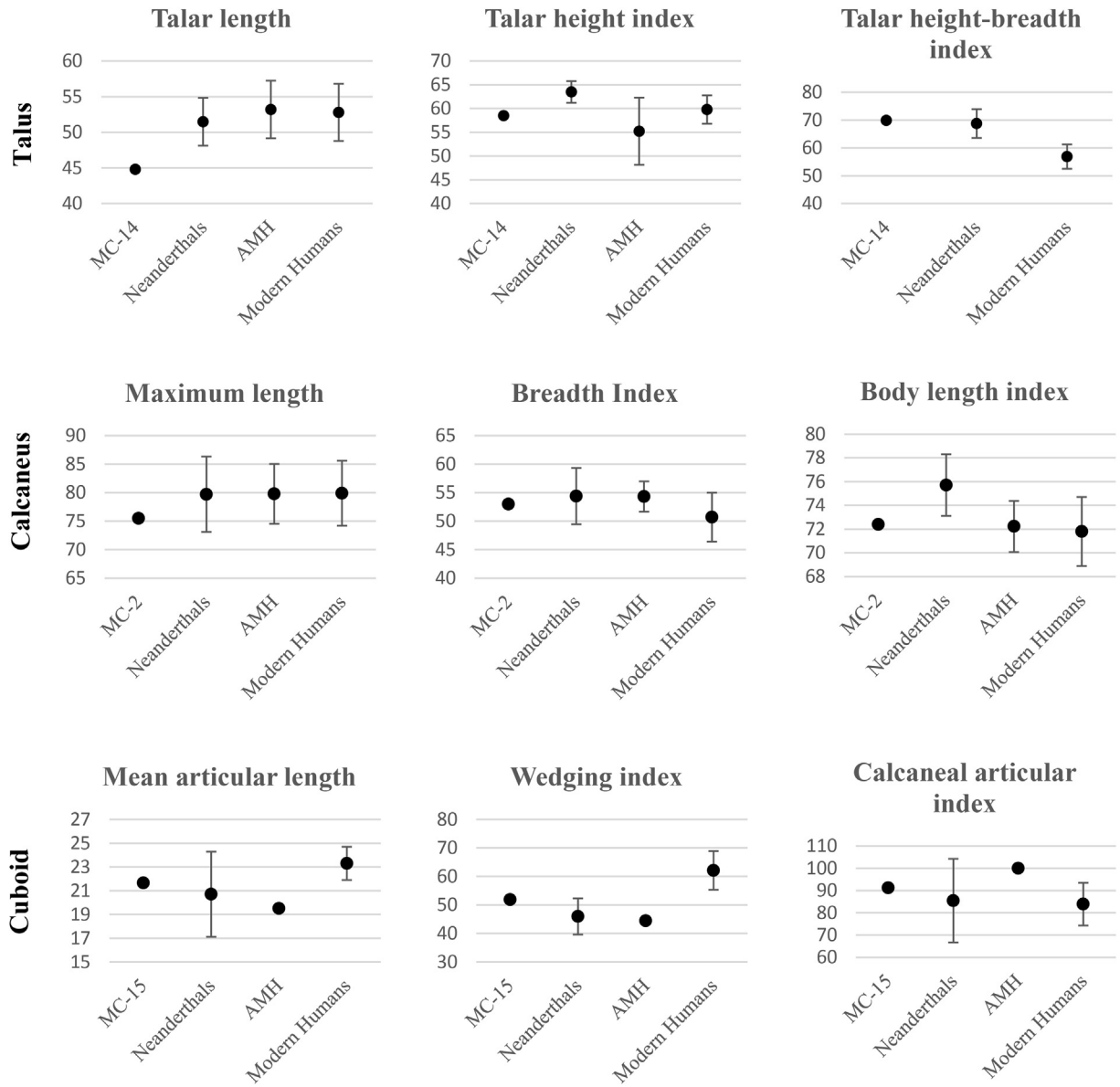

Figure 7. Error bar charts representing the mean and standard deviation of one linear measure and two indices for the calcaneus, the talus, and the cuboid for each population group: Manot Cave (MC), Neanderthals, Anatomically Modern Humans (AMH), and modern humans (data in SOM Tables S5–S7).

and AMH (75.7 ± 6.83 mm, n = 4) (Fig. 8; SOM Table S10). Both the DP midshaft diameter and the ML diameter fall within the range of Neanderthals and AMH (SOM Table S10). Its robusticity index falls within the range of variations of the other hominin groups (Fig. 8; SOM Table S10). The sizes of the proximal epiphysis and the proximal articular index are the smallest of the hominin groups, yet the size and articular index of the distal epiphysis is within the range of other hominin groups (Fig. 9; SOM Table S10).

4.5. Pathology

Several indicators of pathology were identified in the second metatarsal (MC-4). These include a dislocation of the plantar third of the base (Fig. 9A), the presence of an irregular bone flake on the dorsomedial surface of the shaft (Fig. 9B), and a healed fracture on the lateral side of the base of the metatarsal (Fig. 9C).

The flake suggests a remote traumatic fracture of the cortical surface, most likely owing to forced contact with the hallucal metatarsal. The surface of the bone flake is highly polished, indicating a chronologically remote incident. It is located on the dorsomedial aspect of the shaft, ~20.0 mm from the facet for the medial cuneiform. The flake itself is 8 mm in length. Related to this observation is the displacement and dislocation of the plantar third of the metatarsal base, indicating an avulsion fracture due to traumatically forced tension on the Lisfranc's ligament. This interosseous ligament runs obliquely between the medial cuneiform and the base of the second metatarsal. Its forced avulsion resulted in the displacement and dislocation of the plantar third of the metatarsal base. Subsequent healing of the subluxed fracture elements has resulted in the irregular surface topography of the proximal facet for the intermediate cuneiform (Fig. 9A, black arrows). The fracture line and spatial distortion are clearly evident on the lateral side of the base obliterating the facet for the third metatarsal (Fig. 9C). In addition, there is a slight but palpable transverse “step” across the cuneiform articular surface indicating the misalignment of the two fracture fragments. Also related to this

Please cite this article as: Borgel, S et al., Early Upper Paleolithic human foot bones from Manot Cave, Israel, Journal of Human Evolution, https://doi.org/10.1016/j.jhevol.2019.102668

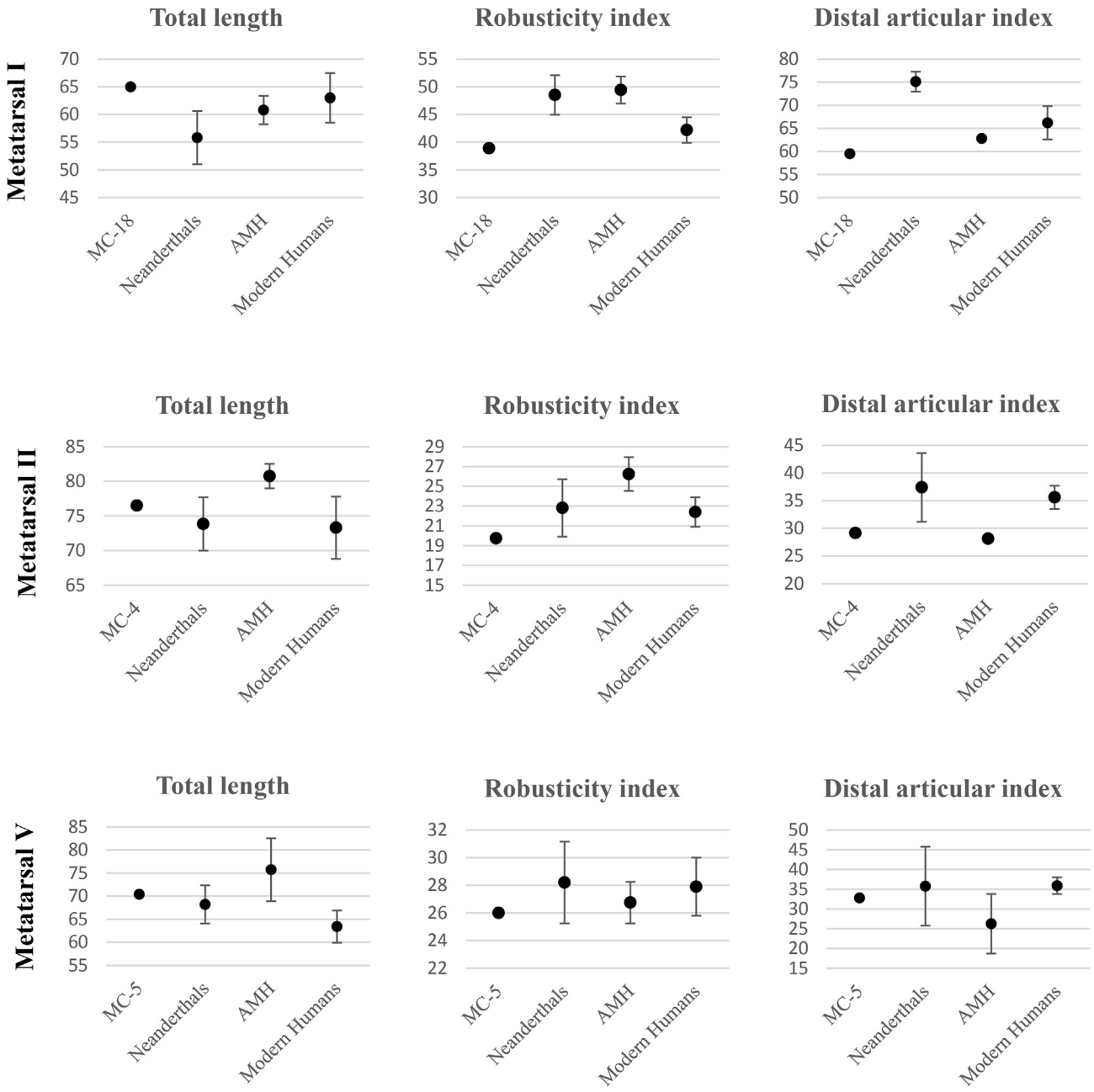

Figure 8. Error bar charts representing the mean and standard deviation of one linear measure and two indices for the first, the second, and the fifth metatarsals for each population group: Manot Cave (MC), Neanderthals, Anatomically Modern Humans (AMH), and modern humans (data in SOM Tables S8–S10).

traumatically produced fracture are the elevated margin of the superior articular facet for the third metatarsal and the lytic excavation of the bone surrounding the facet. The healing process is clearly visible on the μCT image (Fig. 9D). Further evidence of the traumatic event is seen on the medial side of the metatarsal base where the articulation for the medial cuneiform has a depressed concavity in the joint's center and raised circum-articular margins (Fig. 9B).

5. Discussion

The feet of *Homo sapiens* and Neanderthals, although similar in their overall dimensions (Rhoads and Trinkaus, 1977; Trinkaus and Hilton, 1996; Pablos et al., 2017), exhibit some notable differences. These dissimilarities are evident in the morphological and metrical comparison of Manot Cave foot remains with Neanderthals, AMH, and modern humans. Most characteristics of the Manot Cave pedal bones resemble a modern human foot although some features are more similar to Neanderthals.

The Manot Cave talus, similar to modern humans, has a relatively long head-neck as opposed to AMH and Neanderthals (Trinkaus, 1975; Pablos et al., 2013; Rosas et al., 2017). The talar trochlea is not rectangular as in Neanderthals (parallel medial and lateral margins) (Pablos et al., 2013), but rather has a frustum shape (a smaller radius of curvature on the medial side), similar to modern humans. The Manot Cave talus has a narrow relative articular breadth as well as a narrow posterior calcaneal articular surface when compared with Neanderthals. These surfaces are

Please cite this article as: Borgel, S et al., Early Upper Paleolithic human foot bones from Manot Cave, Israel, Journal of Human Evolution, https://doi.org/10.1016/j.jhevol.2019.102668

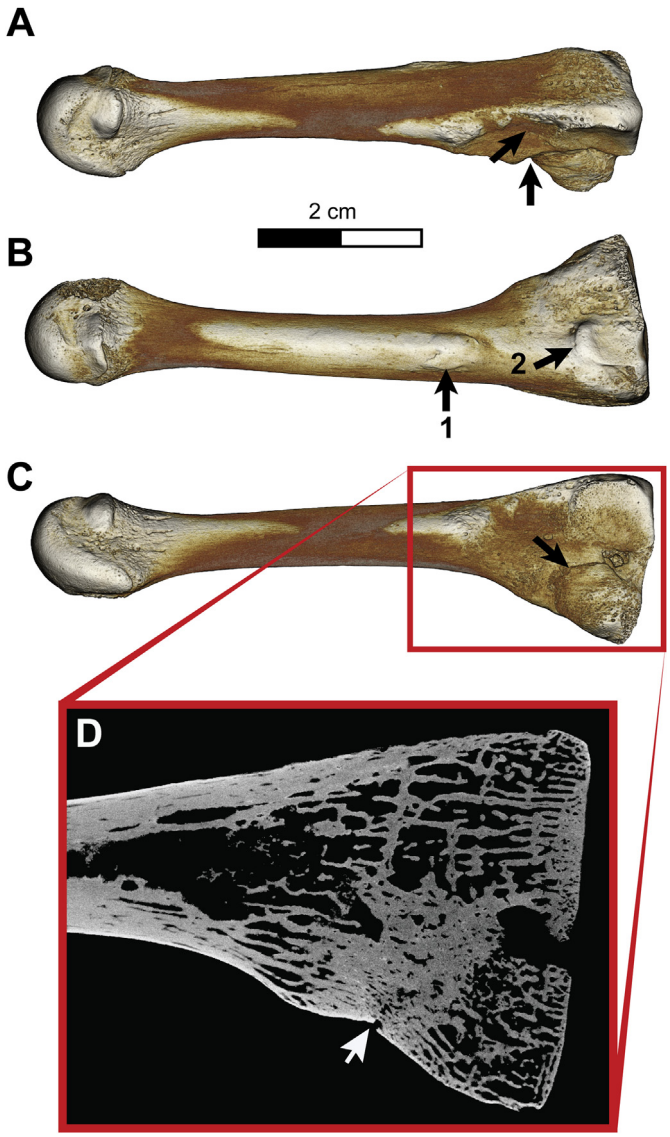

Figure 9. Images of the μCT reconstruction of the Manot Cave second metatarsal. (A) Dorsolateral view, the black arrows show the unusual topography of the proximal epiphysis; (B) Medial view with (1) the flake and (2) the raised medial margin on the medial articular facet; (C) The fracture line on the lateral side of the proximal epiphysis, and (D) The sagittal section at the fracture's level (white arrow pointing at the fracture line).

associated with a higher body-mass index, higher biomechanical stress, and a greater post-cranial robustness than seen in Neanderthals (Trinkaus, 1975; Rhoads and Trinkaus, 1977; Lorenzo et al., 1999; Harcourt-Smith and Aiello, 2004; Lu et al., 2011; Rosas et al., 2017). The Manot Cave talar trochlea is remarkably tall relative to its length when compared with the other hominins examined. A tall talar trochlea is considered a characteristic of modern humans (Boyle and DeSilva, 2015; McNutt et al., 2018) that enables a relatively greater capacity for dorsiflexion and plantarflexion of the talocrural ankle joint (Barnett and Napier, 1952; Gebo and Schwartz, 2006), though the reason for this ability is unknown (DeSilva et al., 2019). The lateral malleolar facet of Manot Cave talus is relatively broad, falling within the upper range of Neanderthals. Although this trait was previously suggested as a Neanderthal trait (Rhoads and Trinkaus, 1977; Pablos et al., 2013), in our study both Manot Cave and the Neanderthals fell within the variation of modern humans.

In general, the calcaneus of Manot Cave also manifests modern human proportions; the body is relatively short, the posterior talar articular surface is relatively narrow, and the insertion area for the triceps surae tendon is modestly developed. Neanderthals, in contrast, display a robust and long calcaneus, a mediolaterally wide tuber, and expanded articular surfaces (Rhoads and Trinkaus, 1977; Schmitt, 1998; Pablos et al., 2014, 2017; DeSilva et al., 2019). The elongated calcaneal body of Neanderthals is related to more efficient walking, yet lower endurance while running (DeSilva et al., 2019). Two features in the Manot Cave calcaneus are considered similar to Neanderthals; the tall body (Nogueira et al., 2017), and the robust sustentaculum tali (Pablos et al., 2014; DeSilva et al., 2019).

The Manot Cave cuboid morphology is similar to that of modern humans, with a longer lateral border compared with AMH and Neanderthals, but with a wedging index intermediate between Neanderthals and modern humans. The Manot Cave cuboid is notable because of its diminutive plantar tuberosity and its moderately excavated groove for the peroneus longus tendon; both features are most often seen in the cuboids of modern humans (McCown and Keith, 1939). The first metatarsal of Manot Cave is, in most dimensions, similar to that of modern humans (i.e., long and narrow). In contrast, Neanderthals display a relatively short and robust first metatarsal (Trinkaus, 1975). The Manot Cave fifth metatarsal is more Neanderthal-like, with a slightly greater length than that of modern humans (Trinkaus, 1975). The Manot Cave second metatarsal is similar in length to that of Neanderthals and modern humans. This is consistent with previous findings indicating that the second metatarsal does not differ in length between these two groups (Trinkaus, 1975). A unique feature of the Manot Cave metatarsals is the small size of their distal articular surface relative to the metatarsal length (i.e., the distal articular index), particularly in the first and second metatarsals.

To summarize, the Manot Cave foot bones are similar to those of modern humans in their overall general appearance and their remarkable gracility (Ruff et al., 1993; Ryan and Shaw, 2015), with the exception of a slightly taller calcaneal body, a projected sustentaculum tali and a somewhat longer fifth metatarsal, both of which fall within Neanderthal ranges of variation. In addition, the Manot Cave specimen displays a uniquely small talus and calcaneus when compared with the long metatarsals. The Neanderthal foot bones, in contrast, are characterized by their enhanced robustness, especially evident in the talus and the first and fifth metatarsals (Trinkaus, 1975; Mersey et al., 2013). The AMH foot bones, best represented by fossils from Skhul and Qafzeh (~120-90kyr ago) display an intermediate robusticity between modern humans and Neanderthals (McCown and Keith, 1939; Vandermeersch, 1981).

The injury seen on the second metatarsal provides evidence of a localized, remote traumatic fracture. The apparent sequelae include the polished bone flake adherent to the shaft, the significant remodeling, distortion of the fractured base, the anatomical misalignment of the broken elements, and the osseous reaction surrounding the bone's base. These observations provide strong evidence that this individual suffered a traumatic injury to his/her midfoot, most likely what in modern medical terminology would be referred to as a Lisfranc's fracture (Kalia et al., 2012). Also associated with the original injury and the subsequent residual ligamentous instability are the subtle articular reactions throughout the associated pedal elements. Such lesions are commonly found in a fracture/dislocation of one or more of the metatarsals from the tarsus (Welck et al., 2015; Lau et al., 2016).

The mechanism underlying Lisfranc's injury in children differs from that of adults. Whereas in children it commonly occurs during a fall from a height (Johnson, 1981), in adults it usually occurs due to a direct force (traumatic crush fracture) applied to the dorsum of

Please cite this article as: Borgel, S et al., Early Upper Paleolithic human foot bones from Manot Cave, Israel, Journal of Human Evolution, https://doi.org/10.1016/j.jhevol.2019.102668

the mid-foot, or an indirect force due to excessive pronation or supination in a plantarflexed foot (Coetzee, 2008). The latter is quite rare (Desmond and Chou, 2006), except for athletes (Benirschke et al., 2012). Lisfranc's injury is a frequent injury in children (Johnson, 1981), and it commonly affects the second metatarsal (van Rijn et al., 2012; Welck et al., 2015). Males are at a higher risk (two to four times) to suffer from it, possibly due to a higher rate of participation in high-energy activities (Welck et al., 2015). Patients with this injury limp and walk on the lateral margin of the foot. In children, this fracture heals rather quickly (two to three weeks) (Johnson, 1981); however, in adults, recovery takes about six weeks (Nunley and Vertullo, 2002).

To the best of our knowledge, Lisfranc's fracture has never been reported in a prehistoric population. A few examples of prehistoric pedal bones injuries have been published and include a healed compression fracture of the talus of *Australopithecus africanus* (Fisk and Macho, 1992), a healed stress fracture of the fourth metatarsal of *H. antecessor* (Martin-Francés et al., 2015), and a periosteal lesion of traumatic origin in a fourth metatarsal from the Sima de los Huesos site (Gracia-Téllez et al., 2012). Neanderthal skeletal evidence of foot injuries includes a healed fracture of the diaphysis of the fifth metatarsal of Shanidar 1 (Trinkaus and Zimmerman, 1982), a healed fracture on the diaphysis of the fifth right proximal phalanx, osteophytes on the talus and intermediate cuneiform bone of the Neanderthal specimen of Kiik-Koba 1 (Trinkaus et al., 2008), and a severe degenerative joint disease and arthritic reaction on the talocrural and talocalcaneal articulations of Shanidar 3 and Shanidar 1 (Trinkaus and Zimmerman, 1982; Berger and Trinkaus, 1995). Such injuries must have impacted the locomotion of the injured individual, and their long-term survival suggests that they lived within a supportive social system (Trinkaus and Zimmerman, 1982). Further evidence for similar social support among hominins can be found in the survival of Shanidar 3 who suffered from a penetrating wound in the thorax (Trinkaus and Zimmerman, 1982), the survival of a toothless individual from Dmanisi (D3444/D3900) (Lordkipanidze et al., 2005), and the healed lesion on the frontal bone of the Middle Pleistocene Maba 1 specimen (Wu et al., 2011). Following the original traumatic incident, the young individual from Manot Cave would have suffered from pain and restricted mobility. Recovering from such an injury, as this young individual did, could only be possible within a supportive community.

Among the Early Upper Paleolithic population in Europe, evidence exists not only for supporting invalid individuals during their lifetime, but also for granting them special treatment after death. These funerary behaviors are evident in the triple burial from Dolní Věstonice (Formicola et al., 2001), and the double burial from Sunghir (Formicola and Buzhilova, 2004). In the Natufian site of Hilazon, a burial of an old woman with several pathologies was interpreted as a burial of a Shaman (Grosman et al., 2008). The association of the Manot Cave pedal foot along with unique findings, such as marine mollusks and a large and exclusive flint assemblage (Abulafia et al., submitted) may be evidence that they were used as burial offerings, thus concluding that the Manot Cave people gave special attention to their dead.

Acknowledgments

This work was supported by the Dan David Foundation, The Shmunis Family Anthropology Institute, Binational Science Foundation, Israel and United States (grant no. 2015303), Israel Science Foundation (grant no. 2632/18), The Leakey Foundation and the Shafran Family Foundation. This work was performed in partial fulfillment of the requirements for a Ph.D. degree by Sarah Borgel at the Sackler Faculty of Medicine, Tel Aviv University, Israel.

Supplementary Online Material

Supplementary online material to this article can be found online at https://doi.org/10.1016/j.jhevol.2019.102668.

References

Abulafia, T., Goder-Golderger, M., Berna, F., Barzilai, O., Marder, O., 2019. A techno-typological analysis of the Ahmarian and Levantine Aurignacian assemblages from Manot Cave (Area C) and the interrelation with the formation processes. Journal of Human Evolution [in press].

Alex, B., Barzilai, O., Hershkovitz, I., Marder, O., Berna, F., Caracuta, V., Abulafia, T., Davis, L., Goder-Golberger, M., Lavi, R., Mintz, E., Regev, L., Bar-Yosef Mayer, D., Tejero, J.M., Yeshurun, R., Ayalon, A., Bar-Matthews, M., Yasur, G., Frumkin, A., Latimer, B., Hans, M.G., Boaretto, E., 2017. Radiocarbon chronology of Manot Cave, Israel and Upper Paleolithic dispersals. Science Advances 3, e1701450.

Barnett, C.H., Napier, J.R., 1952. The axis of rotation at the ankle joint in man. Its influence upon the form of the talus and the mobility of the fibula. Journal of Anatomy 86, 1–9.

Bar-Yosef, O., 2002. The Upper Paleolithic revolution. Annual Review of Anthropology 31, 363–393.

Bar-Yosef, O., 2007. The archaeological framework of the Upper Paleolithic revolution. Diogenes 54, 3–18.

Bar-Yosef Mayer, D., 2019. Upper Paleolithic explorers: the geographic sources of shell beads in Early Upper Paleolithic assemblages in Israel. PaleoAnthropology 2019, 105–115.

Barzilai, O., Hershkovitz, I., Marder, O., 2016. The Early Upper Paleolithic period at Manot Cave, Western Galilee, Israel. Human Evolution 31, 85–100.

Benirschke, S.K., Meinberg, E., Anderson, S.A., Jones, C.B., Cole, P.A., 2012. Fractures and dislocations of the midfoot: Lisfranc and Chopart injuries. The Journal of Bone & Joint Surgery 94, 1325–1337.

Berger, T.D., Trinkaus, E., 1995. Patterns of trauma among the Neandertals. Journal of Archaeological Science 22, 841–852.

Bergman, C.A., Stringer, C.B., 1989. Fifty years after: Egbert, an Early Upper Palaeolithic juvenile from Ksar Akil. Paléorient, Lebanon, pp. 99–111.

Betti, L., Lycett, S.J., von Cramon-Taubadel, N., Pearson, O.M., 2015. Are human hands and feet affected by climate? A test of Allen's rule. American Journal of Physical Anthropology 158, 132–140.

Bojsen-Møller, F., 1979. Calcaneocuboid joint and stability of the longitudinal arch of the foot at high and low gear push off. Journal of Anatomy 129, 165–176.

Boyle, E., DeSilva, J.M., 2015. A large *Homo erectus* talus from Koobi for a, Kenya (KNM-ER 5428), and Pleistocene hominin talar evolution. Paleoanthropology 2015, 1–13.

Byers, S., Akoshima, K., Curran, B., 1989. Determination of adult stature from metatarsal length. American Journal of Physical Anthropology 79, 275–279.

Cardoso, H.F.V., Severino, R.S.S., 2010. The chronology of epiphyseal union in the hand and foot from dry bone observations. International Journal of Osteoarchaeology 20, 737–746.

Coetzee, J.C., 2008. Making sense of Lisfranc injuries. Foot and Ankle Clinics 13, 695–704.

Day, M.H., Wood, B.A., 1968. Functional affinities of the Olduvai Hominid 8 talus. Man 3, 440–455.

DeSilva, J.M., 2009. Functional morphology of the ankle and the likelihood of climbing in early hominins. Proceedings of the National Academy of Sciences 106, 6567–6572.

DeSilva, J.M., Zipfel, B., Van Arsdale, A.P., Tocheri, M.W., 2010. The Olduvai Hominid 8 foot: adult or subadult? Journal of Human Evolution 58, 418–423.

DeSilva, J., McNutt, E., Benoit, J., Zipfel, B., 2019. One small step: A review of Plio-Pleistocene hominin foot evolution. American Journal of Physical Anthropology 168, 63–140.

Desmond, E.A., Chou, L.B., 2006. Current concepts review: Lisfranc injuries. Foot & Ankle International 27, 653–660.

Donahue, S.W., Sharkey, N.A., 1999. Strains in the metatarsals during the stance phase of gait: implications for stress fractures. Journal of Bone and Joint Surgery 81, 1236–1244.

Donahue, S.W., Sharkey, N.A., Modanlou, K.A., Sequeira, L.N., Martin, R.B., 2000. Bone strain and microcracks at stress fracture sites in human metatarsals. Bone 27, 827–833.

Douka, K., Bergman, C.A., Hedges, R.E., Wesselingh, F.P., Higham, T.F., 2013. Chronology of Ksar Akil (Lebanon) and implications for the colonization of Europe by anatomically modern humans. PLoS One 8, e72931.

Fisk, G.R., Macho, G.A., 1992. Evidence of a healed compression fracture in a Plio-Pleistocene hominid talus from Sterkfontein, South Africa. International Journal of Osteoarchaeology 2, 325–332.

Formicola, V., Pontrandolfi, A., Svoboda, J., 2001. The Upper Paleolithic triple burial of Dolní Věstonice: Pathology and funerary behavior. American Journal of Physical Anthropology 115, 372–379.

Formicola, V., Buzhilova, A.P., 2004. Double child burial from Sunghir (Russia): Pathology and inferences for Upper Paleolithic funerary practices. American Journal of Physical Anthropology 124, 189–198.

Gebo, D.L., Schwartz, G.T., 2006. Foot bones from Omo: implications for hominid evolution. American Journal of Physical Anthropology 129, 499–511.

Gilead, I., 1991. The Upper Paleolithic period in the Levant. Journal of World Prehistory 5, 105–154.
Gracia-Téllez, A., Pablos, A., Lorenzo, C., Martínez, I., Carretero, J.M., Arsuaga, J.L., 2012. Stress in a Middle Pleistocene hominid (Atapuerca, Spain): periosteal reaction compatible with fatigue fracture in a metatarsal bone. In: Abstracts of 39th Annual Meeting of the Paleopathology Association, Portland (Oregon – USA), 43.
Grosman, L., Munro, N.D., Belfer-Cohen, A., 2008. A 12,000-year-old Shaman burial from the southern Levant (Israel). In: Proceedings of the National Academy of Sciences 105, pp. 17665–17669.
Harcourt-Smith, W.E., Aiello, L.C., 2004. Fossils, feet and the evolution of human bipedal locomotion. Journal of Anatomy 204, 403–416.
Hershkovitz, I., Speirs, M.S., Frayer, D., Nadel, D., Wish-Baratz, S., Arensburg, B., 1995. Ohalo II H2: A 19,000-year-old skeleton from a water-logged site at the Sea of Galilee, Israel. American Journal of Physical Anthropology 96, 215–234.
Hershkovitz, I., Marder, O., Ayalon, A., Bar-Matthews, M., Yasur, G., Boaretto, E., Caracuta, V., Alex, B., Frumkin, A., Goder-Goldberger, M., Gunz, P., Holloway, R.L., Latimer, B., Lavi, R., Matthews, A., Slon, V., Bar-Yosef Mayer, D., Berna, F., Bar-Oz, G., Yeshurun, R., May, H., Hans, M.G., Weber, G.W., Barzilai, O., 2015. Levantine cranium from Manot Cave (Israel) foreshadows the first European modern humans. Nature 520, 216–219.
Hoerr, N.L., Pyle, S.I., Francis, C.C., 1962. Radiographic Atlas of Skeletal Development of the Foot and Ankle: A Standard of Reference. C.C. Thomas, Springfield.
Holland, T.D., 1995. Estimation of adult stature from the calcaneus and talus. American Journal of Physical Anthropology 96, 315–320.
Hublin, J.J., 2015. The modern human colonization of western Eurasia: when and where? Quaternary Science Reviews 118, 194–210.
Johnson, G.F., 1981. Pediatric Lisfranc injury:" bunk bed" fracture. American Journal of Roentgenology 137, 1041–1044.
Kalia, V., Fishman, E.K., Carrino, J.A., Fayad, L.M., 2012. Epidemiology, imaging, and treatment of Lisfranc fracture-dislocations revisited. Skeletal Radiology 41, 129–136.
Kuhn, S.L., Stiner, M.C., Güleç, E., Özer, I., Yılmaz, H., Baykara, I., Açıkkol, A., Goldberg, P., Molina, K.M., Ünay, E., Suata-Alpaslan, F., 2009. The early Upper Paleolithic occupations at Üçağızlı Cave (Hatay, Turkey). Journal of Human Evolution 56, 87–113.
Latimer, B., Ohman, J.C., Lovejoy, C.O., 1987. Talocrural joint in African hominoids: implications for *Australopithecus afarensis*. American Journal of Physical Anthropology 74, 155–175.
Latimer, B., Lovejoy, C.O., 1989. The calcaneus of *Australopithecus afarensis* and its implications for the evolution of bipedality. American Journal of Physical Anthropology 78, 369–386.
Latimer, B., Lovejoy, C.O., 1990. Hallucal tarsometatarsal joint in *Australopithecus afarensis*. American Journal of Physical Anthropology 82, 125–133.
Lau, S., Bozin, M., Thillainadesan, T., 2016. Lisfranc fracture dislocation: a review of a commonly missed injury of the midfoot. Emergency Medicine Journal 34, 52–56.
Lordkipanidze, D., Vekua, A., Ferring, R., Rightmire, G.P., Agusti, J., Kiladze, G., Mouskhelishvili, A., Nioradze, M., de León, M.S.P., Tappen, M., Zollikofer, C.P., 2005. Anthropology: the earliest toothless hominin skull. Nature 434, 717–718.
Lorenzo, C., Arsuaga, J.L., Carretero, J.M., 1999. Hand and foot remains from the Gran Dolina early Pleistocene site (Sierrade Atapuerca, Spain). Journal of Human Evolution 37, 501–522.
Lovejoy, C.O., Latimer, B., Suwa, G., Asfaw, B., White, T.D., 2009. Combining prehension and propulsion: the foot of *Ardipithecus ramidus*. Science 326, 72e1–72e8.
Lu, Z., Meldrum, D.J., Huang, Y., He, J., Sarmiento, E.E., 2011. The Jinniushan hominin pedal skeleton from the late Middle Pleistocene of China. HOMO 62, 389–401.
Mahato, N.K., Murthy, S.N., 2012. Articular and angular dimensions of the talus: inter-relationship and biomechanical significance. The Foot 22, 85–89.
Marder, O., Alex, B., Ayalon, A., Bar-Matthews, M., Bar-Oz, G., Bar-Yosef Mayer, D., Berna, F., Boaretto, E., Caracuta, V., Frumkin, A., Goder-Goldberger, M., Hershkovitz, I., Latimer, B., Lavi, R., Matthews, A., Weiner, S., Weiss, U., Yas'ur, G., Yeshurun, R., Barzilai, O., 2013. The Upper Paleolithic of Manot Cave, western Galilee, Israel: The 2011-12 excavations. Antiquity 87, 1–7.
Marder, O., Barzilai, O., Abulafia, T., Hershkovitz, I., Goder-Goldberger, M., 2018. Chronocultural considerations of Middle Paleolithic occurrences at Manot Cave (Western Galilee), Israel. In: Akazawa, T., Bar-Yosef, O. (Eds.), The Middle and Upper Paleolithic Archeology of the Levant and Beyond. Springer, Singapore, pp. 49–63.
Martin-Francés, L., Martinon-Torres, M., Gracia-Téllez, A., Bermúdez de Castro, J.M., 2015. Evidence of stress fracture in a *Homo antecessor* metatarsal from Gran Dolina Site (Atapuerca, Spain). International Journal of Osteoarchaeology 25, 564–573.
McCown, T.D., Keith, A., 1939. The Stone Age of Mount Carmel. Clarendon Press, Oxford.
McNutt, E.J., Zipfel, B., DeSilva, J.M., 2018. Evolution of the human foot. Evolutionary Anthropology 27, 197–217.
Mellars, P., 2004. Neanderthals and the modern human colonization of Europe. Nature 432, 461–465.
Mellars, P., 2006. Going east: new genetic and archaeological perspectives on the modern human colonization of Eurasia. Science 313, 796–800.
Mersey, B., Jabbour, R.S., Brudvik, K., Defleur, A., 2013. Neanderthal hand and foot remains from Moula-Guercy, Ardèche, France. American Journal of Physical Anthropology 152, 516–529.
Nogueira, D.C., Santos, F., Courtaud, P., Couture-Veschambre, C., 2017. Le calcanéus «Regourdou 2»: étude morphométrique comparative et discussion autour de sa place dans la variabilité des Néandertaliens. PALEO. Revue d'Archéologie Préhistorique 28, 71–89.
Nunley, J.A., Vertullo, C.J., 2002. Classification, investigation, and management of midfoot sprains: Lisfranc injuries in the athlete. American Journal of Sports Medicine 30, 871–878.
Pablos, A., Lorenzo, C., Martínez, I., de Castro, J.M.B., Martinón-Torres, M., Carbonell, E., Arsuaga, J.L., 2012. New foot remains from the Gran Dolina-TD6 Early Pleistocene site (Sierra de Atapuerca, Burgos, Spain). Journal of Human Evolution 63, 610–623.
Pablos, A., Martínez, I., Lorenzo, C., Gracia, A., Sala, N., Arsuaga, J.L., 2013. Human talus bones from the Middle Pleistocene site of Sima de los Huesos (Sierra de Atapuerca, Burgos, Spain). Journal of Human Evolution 65, 79–92.
Pablos, A., Martínez, I., Lorenzo, C., Sala, N., Gracia-Téllez, A., Arsuaga, J.L., 2014. Human calcanei from the Middle Pleistocene site of Sima de los Huesos (Sierra de Atapuerca, Burgos, Spain). Journal of Human Evolution 76, 63–76.
Pablos, A., Pantoja-Pérez, A., Martínez, I., Lorenzo, C., Arsuaga, J.L., 2017. Metric and morphological analysis of the foot in the Middle Pleistocene sample of Sima de los Huesos (Sierra de Atapuerca, Burgos, Spain). Quaternary International 433, 103–113.
Pearson, O.M., 2000. Activity, climate and postcranial robusticity. Current Anthropology 41, 569–607.
Rhoads, J.G., Trinkaus, E., 1977. Morphometrics of the Neandertal talus. American Journal of Physical Anthropology 46, 29–43.
Rosas, A., Ferrando, A., Bastir, M., García-Tabernero, A., Estalrrich, A., Huguet, R., Garcia-Martinez, D., Pastor, J.F., de la Rasilla, M., 2017. Neandertal talus bones from El Sidrón site (Asturias, Spain): A 3D geometric morphometrics analysis. American Journal of Physical Anthropology 164, 394–415.
Ruff, C.B., Trinkaus, E., Walker, A., Larsen, C.S., 1993. Postcranial robusticity in *Homo*. I: Temporal trends and mechanical interpretation. American Journal of Physical Anthropology 91, 21–53.
Ryan, T.M., Shaw, C.N., 2015. Gracility of the modern *Homo sapiens* skeleton is the result of decreased biomechanical loading. Proceedings of the National Academy of Sciences 112, 372–377.
Sarig, R., Fornai, C., Pokhojaev, A., May, H., Hans, M., Marder, O., Barzilay, O., Quam, R., Weber, G.W., 2019. The dental remains from the Early Upper Paleolithic of Manot Cave, Israel. Journal of Human Evolution in press.
Scheuer, L., Black, S., 2004. The Juvenile Skeleton. Elsevier Academic Press, London.
Schmitt, A., 1998. Approche de la variabilité du calcanéus néandertalien. Comparaison avec l'homme moderne. Bulletins et Mémoires de la Société d'Anthropologie de Paris 10, 273–292.
Shea, J.J., 2007. Behavioral differences between Middle and Upper Paleolithic *Homo sapiens* in the East Mediterranean Levant: the roles of intraspecific competition and dispersal from Africa. Journal of Anthropological Research 63, 449–488.
Tejero, J.M., Yeshurun, R., Barzilai, O., Goder-Goldberger, M., Hershkovitz, I., Lavi, R., Schneller-Pels, N., Marder, O., 2016. The osseous industry from Manot Cave (Western Galilee, Israel): Technical and conceptual behaviors of bone and antler exploitation in the Levantine Aurignacian. Quaternary International 403, 90–106.
Trinkaus, E., 1975. A functional analysis of the Neanderthal foot. Ph.D. Dissertation. University of Pennsylvania.
Trinkaus, E., Zimmerman, M.R., 1982. Trauma among the Shanidar Neandertals. American Journal of Physical Anthropology 57, 61–76.
Trinkaus, E., Hilton, C.E., 1996. Neandertal pedal proximal phalanges: diaphyseal loading patterns. Journal of Human Evolution 30, 399–425.
Trinkaus, E., Maley, B., Buzhilova, A.P., 2008. Brief communication: Paleopathology of the Kiik-Koba 1 Neandertal. American Journal of Physical Anthropology 137, 106–112.
Vandermeersch, B., 1981. Les Hommes Fossiles de Qafzeh (Israël). Editions du Centre National de la Recherche Scientifique, Paris.
van Rijn, J., Dorleijn, D.M., Boetes, B., Wiersma-Tuinstra, S., Moonen, S., 2012. Missing the Lisfranc fracture: a case report and review of the literature. Journal of Foot and Ankle Surgery 51, 270–274.
Welck, M.J., Zinchenko, R., Rudge, B., 2015. Lisfranc injuries. Injury 46, 536–541.
Wu, X.J., Schepartz, L.A., Liu, W., Trinkaus, E., 2011. Antemortem trauma and survival in the late Middle Pleistocene human cranium from Maba, South China. Proceedings of the National Academy of Sciences 108, 19558–19562.

Please cite this article as: Borgel, S et al., Early Upper Paleolithic human foot bones from Manot Cave, Israel, Journal of Human Evolution, https://doi.org/10.1016/j.jhevol.2019.102668